terization of the complexes included in this report shows structural properties that may be anticipated for PhD-bridged species. Redox properties show that the semiquinone form of the bridging PhD diolate ligand is readily accessible. We have found, in accord with Abruna's results,[6] that the free PhD ligand undergoes reductions to semiquinone and catecholate forms in two steps at −0.884 and −1.74 V (Fc/Fc$^+$). Coordination of PhD through nitrogen atoms in Ru(bpy)$_2$(*N',N*-PhD)$^{2+}$ results in a positive shift in these potentials to −0.504 and −1.261 V. Our electrochemical study on $(PPh_3)_2Pt(O',O\text{-PhD})$ (Table VI) shows that there is a further positive shift for the ligand coordinated in its diolate form. As a bridging ligand coordinated through both nitrogen and oxygen atoms, these potentials were shifted to the further positive potentials listed in Table VI, reflecting the increased stability of the catecholate form upon coordination. The oxidation potentials of coordinated catecholate ligands are typically found at much more positive potentials than the corresponding potentials of the benzoquinone ligand in free form, often with shifts that are greater than 1.0 V.[2] For PhD, the shift from free ligand to $(PPh_3)_2Pt(O',O\text{-PhD-}N,N')Pt(DBCat)$ is nearly 2 V, and the electrochemical activity of the bridge occurs at potentials that are within the range of accessible redox states of metal ions. This is an important difference between the PhD-bridged species and corresponding bipyridine analogues. At the same time, it opens the opportunity for studies on the nature of bimetallic interactions through the bridge as a function of bridge charge and electronic structure.

Acknowledgment. This research was supported by the National Science Foundation under Grant CHE 88-09923. Palladium, platinum, and ruthenium salts were provided by Johnson Matthey, Inc., through their Metal Loan Program.

Supplementary Material Available: For $(PPh_3)_2Pt(O',O\text{-PhD-}N,N')PdCl_2$ and $(PPh_3)_2Pt(O',O\text{-PhD-}N,N')Ru(PPh_3)_2Cl_2$, tables giving crystal data and details of the structure determination, atom coordinates, bond lengths and angles, anisotropic thermal parameters, and hydrogen atom locations (30 pages); listings of structure factors (54 pages). Ordering information is given on any current masthead page.

Contribution from the Department of Chemistry, University of South Carolina, Columbia, South Carolina 29208

Cluster Synthesis. 33. New Platinum–Osmium Carbonyl Cluster Complexes from $Pt_2Os_5(CO)_{17}(\mu\text{-H})_6$: Synthesis and Characterization of $PtOs_5(CO)_{15}(\mu_3\text{-S})(\mu\text{-H})_6$, $PtOs_5(CO)_{18}(\mu\text{-H})_4$, and $PtOs_4(CO)_{15}(\mu\text{-H})_2$

Richard D. Adams,* Michael P. Pompeo, and Wengan Wu

Received January 30, 1991

From the reaction of $Pt_2Os_5(CO)_{17}(\mu\text{-H})_6$ with H_2S at 25 °C the new platinum–osmium carbonyl cluster complex $PtOs_5(CO)_{15}(\mu_3\text{-S})(\mu\text{-H})_6$ (**2**) was obtained in 83% yield. Compound **2** was characterized by IR, ^{1}H NMR, ^{13}C NMR, and single-crystal X-ray diffraction analyses. The structure of **2** consists of a $PtOs_3$ tetrahedron fused to a $PtOs_2$ triangle with the platinum atom at the vertex-sharing site. There is a triply bridging sulfido ligand on the $PtOs_2$ triangular grouping. The molecule was shown by variable-temperature ^{1}H NMR and ^{13}C NMR spectroscopy to undergo a dynamic process that involves an intramolecular rotation of the Os_3 triangular group relative to the Os_2S grouping at the platinum atom. ΔG^*_{261} = 12.3 kcal/mol. The reaction of $Pt_2Os_5(CO)_{17}(\mu\text{-H})_6$ with $Os(CO)_5$ at 25 °C yielded two new platinum–osmium carbonyl cluster complexes $PtOs_5(CO)_{18}(\mu\text{-H})_4$ (**3**) and $PtOs_4(CO)_{15}(\mu\text{-H})_2$ (**4**) in 38% and 25% yields, respectively. Both compounds were characterized crystallographically. The cluster of compound **3** consists of a $PtOs_3$ tetrahedron fused to a $PtOs_2$ triangle by the vertex-sharing platinum atom. The cluster of compound **3** contains a $PtOs_3$ tetrahedron with an edge-bridging $Os(CO)_4$ group. The positions of all of the hydride ligands in **3** and **4** were determined by a combination of ^{1}H NMR spectroscopy and crystallography. Compound **3** is readily degraded by CO (25 °C/1 atm) to yield the products $PtOs_2(CO)_{10}$, $H_2Os_2(CO)_8$, and $H_2Os(CO)_4$. Crystal data: for **2**, space group $P\bar{1}$, a = 19.451 (6) Å, b = 23.075 (3) Å, c = 9.771 (2) Å, α = 94.69 (1)°, β = 100.81 (2)°, γ = 98.90 (2)°, Z = 6, 5486 reflections, R = 0.040; for **3**, space group $P2_1$, a = 8.875 (5) Å, b = 19.47 (1) Å, c = 9.370 (3) Å, β = 116.42 (3)°, Z = 2, 1607 reflections, R = 0.045; for **4**, space group $P2_1/c$, a = 13.337 (2) Å, b = 8.809 (3) Å, c = 20.141 (4) Å, β = 90.59 (2)°, Z = 4, 2400 reflections, R = 0.036.

Introduction

The importance of heterobimetallic "clusters" containing platinum as catalysts in the petroleum re-forming process[1] has produced a great interest in the chemistry of heteronuclear cluster complexes containing platinum.[2] We have recently discovered a series of new hydrogen-rich platinum–osmium carbonyl cluster complexes that were obtained from the reaction of $Pt_2Os_4(CO)_{18}$ with hydrogen.[3] Their structures consist of vertex-fused polyhedra with platinum atoms at the vertex-sharing positions. The complex $Pt_2Os_5(CO)_{17}(\mu\text{-H})_6$ (**1**) is a representative member of this series.

We have now investigated the reaction of **1** with H_2S and $Os(CO)_5$. The reactions have yielded the new complexes $PtOs_5(CO)_{15}(\mu_3\text{-S})(\mu\text{-H})_6$ (**2**) and $PtOs_5(CO)_{18}(\mu\text{-H})_4$ (**3**) plus

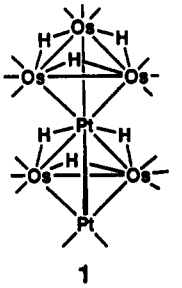

1

$PtOs_4(CO)_{15}(\mu\text{-H})_2$ (**4**), respectively. Details of the preparation, characterization, and reactivity of these compounds toward CO are presented in this report.

Experimental Section

General Procedures. Reactions were performed under a dry nitrogen atmosphere. Reagent grade solvents were dried over sodium and deoxygenated by purging with nitrogen prior to use. $Pt_2Os_5(CO)_{17}(\mu\text{-H})_6$ was prepared by the previously reported procedure.[3] IR spectra were recorded on a Nicolet 5DXB FT-IR spectrophotometer. ^{1}H NMR spectra were recorded on a Bruker AM-300 FT-NMR spectrometer. Natural-abundance ^{13}C NMR spectra were recorded on a Bruker AM-500 FT-NMR

(1) (a) Biswas, J.; Bickle, G. M.; Gray, P. G.; Do, D. D.; Barbier, J. *Catal. Rev.—Sci. Eng.* **1988**, *30*, 161. (b) Sinfelt, J. H. *Bimetallic Catalysts. Discoveries, Concepts and Applications*; John Wiley & Sons: New York, 1983.

(2) (a) Farrugia, L. J. *Adv. Organomet. Chem.* **1990**, *31*, 301. (b) Braunstein, P.; Rose, J. In *Stereochemistry of Organometallic and Inorganic Compounds*; Bernal, I., Ed.; Elsevier: Amsterdam, 1989; Vol. 3.

(3) Adams, R. D.; Pompeo, M. P.; Wu, W. *Inorg. Chem.*, in press.

0020-1669/91/1330-2899$02.50/0

spectrometer operating at 125.7 MHz. Elemental microanalyses were performed by Desert Analytics, Tucson, AZ. TLC separations were performed by using silica gel (60 Å, F_{254}) on plates (Whatman 0.25 mm).

Reaction of $Pt_2Os_5(CO)_{17}(\mu\text{-}H)_6$ (1) with H_2S. A 15.0-mg sample of **1** (0.0082 mmol) was dissolved in CH_2Cl_2 (15 mL), and H_2S was bubbled through the solution slowly at 25 °C for 20 min. The color of the solution changed from dark green to orange-red during this time. The solvent was removed in vacuo, and the residue was separated by TLC on silica gel by using hexane solvent. Only one band, orange-red $PtOs_5(CO)_{15}(\mu_3\text{-}S)(\mu\text{-}H)_6$ (**2**), 11.0 mg (yield 83%), was obtained. IR (ν(CO), cm^{-1}; in hexane): 2116 (vw), 2094 (s), 2087 (s), 2078 (m), 2073 (s), 2033 (sh), 2029 (m), 2021 (w), 2009 (vs), 1996 (w). ^1H NMR (δ; in CD_2Cl_2): at 25 °C, −17.31 (d, 2 H, $^1J_{Pt-H}$ = 572.4 Hz, $^2J_{H-H}$ = 2.7 Hz), −18.76 (s, broad, 3 H, $^2J_{Pt-H}$ = 25 Hz), −20.49 (t, 1 H, $^2J_{H-H}$ = 2.7 Hz); at −80 °C, −17.39 (d, 2 H, $^1J_{Pt-H}$ = 578.7 Hz, $^2J_{H-H}$ = 2.5 Hz), −18.62 (d, 2 H, $^2J_{Pt-H}$ = 25.7 Hz, $^2J_{H-H}$ = 2.1 Hz), −19.07 (t, 1 H, $^2J_{Pt-H}$ = 25.7 Hz, $^2J_{H-H}$ = 2.1 Hz), −20.50 (t, 1 H, $^2J_{H-H}$ = 2.5 Hz). ^{13}C NMR (δ; in $CDCl_3$): at 25 °C, 173.27 (s, br, 3 CO, $^2J_{Pt-C}$ = 34 Hz), 168.19 (s, 2 CO, $^2J_{Pt-C}$ = 19 Hz), 163.95 (s, br, 6 CO), 162.58 (s, 2 CO), 157.19 (s, 2 CO); at −49 °C, 174.69 (s, 1 CO), 173.45 (s, 2 CO), 168.60 (s, 2 CO), 165.15 (s, 2 CO), 164.36 (s, 2 CO), 163.00 (s, 2 CO), 162.79 (s, 2 CO), 157.47 (s, 2 CO). Anal. Calcd (found) for **2**: C, 11.23 (11.56); H, 0.38 (0.32).

Reaction of 1 with $Os(CO)_5$. In a typical reaction, a solution of **1** (8.0 mg, 0.0044 mmol) in hexane (15 mL) was combined with a solution of $Os(CO)_5$ (5.0 mL, 1.6 mg/mL, 0.024 mmol) and the mixture stirred at 25 °C for 1 h. The solvent was removed in vacuo, and the residue was separated by TLC on silica gel with a hexane/CH_2Cl_2 (95/5) solvent mixture. This yielded, in order of elution, 1.5 mg of orange $PtOs_4(CO)_{15}(\mu\text{-}H)_2$ (**4**) (25%), 0.7 mg of red $Pt_2Os_4(CO)_{18}$[4] (10%), and 2.8 mg of red $PtOs_5(CO)_{18}(\mu\text{-}H)_4$ (**3**) (38%). IR (ν(CO), cm^{-1}; in hexane): for **4**, 2091 (s), 2082 (w), 2072 (vs), 2065 (sh), 2057 (w), 2049 (s), 2037 (w), 2032 (m) 2025 (m), 2016 (w), 2009 (w), 2005 (sh), 1990 (vw), 1978 (vw), 1972 (vw); for **3**, 2128 (w), 2103 (w), 2095 (m), 2079 (s), 2070 (vs), 2061 (sh), 2051 (s), 2046 (m), 2030 (w), 2016 (sh), 2009 (m), 2002 (sh), 1994 (w), 1987 (w), 1981 (sh). ^1H NMR (δ): for **4** (at 25 °C; in $CDCl_3$) −20.67 (s, 2 H); for **3** (at −65 °C; in CD_2Cl_2), −17.41 (s, 1 H, $^1J_{Pt-H}$ = 436.0 Hz), −18.09 (s, 1 H, $^1J_{Pt-H}$ = 438.6 Hz), −18.14 (s, 1 H), −18.53 (s, 1 H). Anal. Calc (found) for **3**: C, 13.07 (13.47); H, 0.17 (0.20). Calc (found) for **4**: C, 13.07 (13.16); H, 0.24 (0.25).

Reaction of 3 with CO. The reaction of **3** (1.5 mg) with CO was performed in an NMR tube in 1.0 mL of $CDCl_3$ at 25 °C and was followed by ^1H NMR spectroscopy. After 30 min, the reaction solution contained $H_2Os_2(CO)_8$ and $H_2Os(CO)_4$ in an approximately 2:1 ratio and an intermediate X. After 2 h, the ratio of the three products $H_2Os(CO)_4/H_2Os_2(CO)_8$/X was approximately 2/3/1. Only $H_2Os(CO)_4$ and $H_2Os_2(CO)_8$ were detected in a 1/1 ratio after 4 h. The color of the solution changed from red to yellow. The presence of $PtOs_2(CO)_{10}$[4] was established by IR spectroscopy after chromatography of the sample.

Attempted Reaction of 4 with CO. A 1.5-mg sample of **4** was treated with CO in 1.0 mL of $CDCl_3$ solvent in an NMR tube at 25 °C. No change was detected by ^1H NMR spectroscopy over a period of 21 h.

Attempted Reaction of 2 with CO. A 3.0-mg quantity of **2** was allowed to react with CO in 1.0 mL of $CDCl_3$ solvent in an NMR tube at 25 °C. No reaction was detected by ^1H NMR spectroscopy over a period of 17 h.

Crystallographic Analyses. Crystals of compound **2** were grown by slow evaporation of solvent from a CH_2Cl_2/hexane (1/4) solution at 10 °C. Crystals of compound **3** were grown by slow evaporation of solvent from a CH_2Cl_2/hexane (3/7) solution of 10 °C. Crystals of compound **4** were grown by slow evaporation of solvent from a CH_2Cl_2/hexane (2/3) solution at −20 °C. All data crystals were mounted in thin-walled glass capillaries. Diffraction measurements were made on a Rigaku AFC6S fully automated four-circle diffractometer using graphite-monochromatized Mo Kα radiation. Unit cells were determined and refined from 15 randomly selected reflections obtained by using the AFC6 automatic search, center, index, and least-squares routines. Crystal data, data collection parameters, and results of the analyses are listed in Table I. All data processing was performed on a Digital Equipment Corp. VAXstation 3520 computer by using the TEXSAN structure solving program library (version 5.0) obtained from the Molecular Structure Corp., The Woodlands, TX. Neutral-atom scattering factors were calculated by the standard procedures.[5a] Anomalous dispersion corrections were applied to all non-hydrogen atoms.[5b] Lorentz/polarization (Lp) and absorption corrections were applied to the data for each structure. Full-matrix least-squares refinements minimized the function $\sum_{hkl} w(|F_o| - |F_c|)^2$ where $w = 1/\sigma(F_o)^2$, $\sigma(F_o) = \sigma(F_o^2)/2F_o$, and $\sigma(F_o^2) = [\sigma(I_{raw})^2 + (0.02I_{net}^2)^2]^{1/2}/Lp$.

Table I. Crystal Data for Compounds **2**–**4**

	2	**3**	**4**
formula	$PtOs_5SO_{15}C_{15}H_6$	$PtOs_5O_{18}C_{18}H_4$	$PtOs_4O_{15}C_{15}H_2$
fw	1604.35	1654.31	1378.06
crystal syst	triclinic	monoclinic	monoclinic
a, Å	19.541 (6)	8.875 (5)	13.337 (2)
b, Å	23.075 (3)	19.47 (1)	8.809 (3)
c, Å	9.771 (2)	9.370 (3)	20.141 (4)
α, deg	94.69 (1)	90.0	90.0
β, deg	100.81 (2)	116.42 (3)	90.59 (2)
γ, deg	98.90 (2)	90.0	90.0
V, Å^3	4228 (3)	1450 (1)	2366 (2)
space group	$P\bar{1}$ (No. 2)	$P2_1$ (No. 4)	$P2_1/c$ (No. 14)
Z value	6	2	4
λ(Kα), Å	0.71069	0.71069	0.71069
ρ_{calc}, g/cm^3	3.78	3.79	3.87
μ(Mo Kα), cm^{-1}	276.06	267.77	274.50
transm coeff (max–min)	1.00–0.24	1.00–0.36	0.179–0.004
T, °C	20	20	20
no. of obs ($I > 3\sigma$)	5486	1607	2400
residuals: R, R_w	0.040, 0.038	0.045, 0.047	0.036, 0.041

Compound **2** crystallized in the triclinic crystal system. The space group $P\bar{1}$ was assumed and confirmed by the successful solution and refinement of the structure. The crystal contains 3 formula equiv of **2** in the asymmetric unit. The positions of the metal atoms were obtained by direct methods (MITHRIL). All remaining non-hydrogen atoms were obtained by a series of subsequent difference Fourier syntheses. Due to the large size of the structure, only atoms heavier than carbon were refined with anisotropic thermal parameters. The hydride ligands could not be located and were ignored.

Compounds **3** and **4** crystallized in the monoclinic crystal system. For **3** the systematic absences were consistent with either space group $P2_1$ or $P2_1/m$. A statistical analysis of the intensity distribution indicated a noncentric space group. The space group $P2_1$ was selected and confirmed by the solution and refinement of the structure. The structure was solved by a combination of direct methods (MITHRIL) and difference Fourier syntheses. Only the metal atoms were refined anisotropically. The hydride ligands could not be located and were ignored. When the refinement was completed, the coordinates of all of the atoms were inverted and refined again to establish the enantiomeric form of the molecule. This produced significantly higher residuals of R_w = 0.051 versus R_w = 0.047; thus, the original enantiomeric configuration was retained.

For **4** the space group $P2_1/n$ was identified uniquely on the basis of the systematic absences observed during the collection of data. The structure was solved by a combination of direct methods (MITHRIL) and difference Fourier syntheses. All non-hydrogen atoms were refined with anisotropic thermal parameters. The positions of the hydride ligands were obtained from difference Fourier maps. Their contributions were added to the structure factor calculations, but their positions could not be refined to convergence. Therefore, they were retained as fixed contributions only.

Results

The reaction of **1** with H_2S at 25 °C yielded only one product; $PtOs_5(CO)_{15}(\mu_3\text{-}S)(\mu\text{-}H)_6$ (**2**), 83%. Compound **2** was characterized by a combination of IR, ^1H NMR, ^{13}C NMR, and single-crystal X-ray diffraction analyses. Compound **2** crystallizes in the triclinic crystal system with three symmetry-independent formula units in the unit cell. All three molecules are structurally similar, and an ORTEP diagram of the structure of one of them is shown in Figure 1. Final atomic positional parameters are listed in Table II. Selected interatomic distances and angles are listed in Tables III and IV. The molecule contains one platinum and five osmium atoms. The cluster can be viewed as a combination of one tetrahedral $PtOs_3$ cluster joined to one triangular $PtOs_2$ cluster by a common platinum atom. There is a triply bridging sulfido ligand bridging the $PtOs_2$ triangular group. Each osmium atom contains three linear terminal carbonyl ligands. The molecule is structurally very similar to that of **1** except that it contains a sulfido ligand in place of the $Pt(CO)_2$ grouping. The hydride ligands were not observed in the structural analysis, but

(4) Sundberg, P. *J. Chem. Soc., Chem. Commun.* **1987**, 1307.
(5) (a) *International Tables for X-ray Crystallography*; Kynoch Press: Birmingham, England, 1975; Vol. IV, Table 2.2B, pp 99–101. (b) *Ibid.*, Table 2.3.1, pp 149–150.

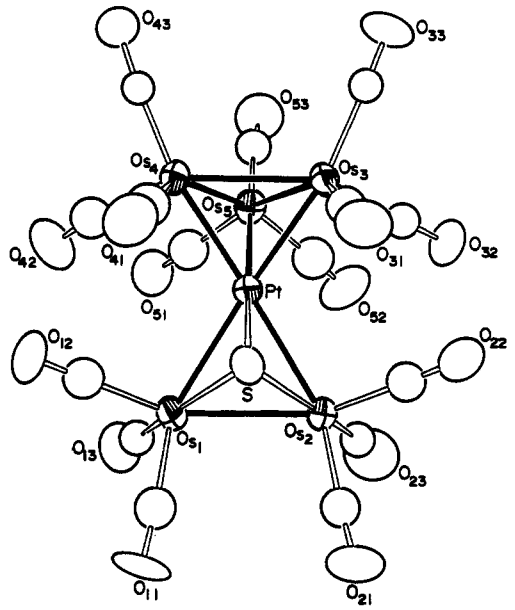

Figure 1. ORTEP diagram of one of the three independent molecules, $PtOs_5(CO)_{15}(\mu_3\text{-}S)(\mu\text{-}H)_6$, in the crystal of **2** showing 50% probability thermal ellipsoids.

the presence of six hydride ligands analogous to those in **1** was established by ^1H NMR spectroscopy. At −80 °C, the ^1H NMR spectrum of **2** shows four resonances: (1) a doublet (2 H) at −17.39 ppm, $^2J_{H\text{-}H}$ = 2.5 Hz with ^{195}Pt satellites indicative of strong Pt–H coupling, $^1J_{Pt\text{-}H}$ = 578.7 Hz; (2) a doublet (2 H) at −18.62 ppm, $^2J_{H\text{-}H}$ = 2.1 Hz with weak coupling to platinum, $^2J_{Pt\text{-}H}$ = 25.7 Hz; (3) a triplet (1 H) at −19.07, $^2J_{H\text{-}H}$ = 2.1 Hz with weak coupling to platinum, $^2J_{Pt\text{-}H}$ = 25.7 Hz; and (4) a triplet (1 H) at −20.50 ppm, $J_{H\text{-}H}$ = 2.5 Hz with no discernible coupling to platinum. These observations are consistent with an arrangement of six bridging hydride ligands as shown in structure **2**.

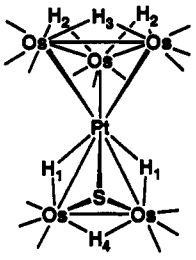

2

This arrangement of hydride ligands which is similar to that for **1** was also indicated indirectly in the structural analysis by the well-known bond-lengthening effects that are produced by bridging hydride ligands.[6] For example, all of the Pt–Os distances to the Os_3 triangle are short, 2.667 (2)–2.702 (2) Å, compared to hydride bridged bonds Pt–Os(1) and Pt–Os(2), 2.886 (2)–2.905 (2) Å. The Os(1)–Os(2) bonds, 2.942 (2)–2.950 (2) Å, and the Os–Os bonds in the Os_3 triangle, 2.890 (2)–2.918 (2) Å, are all long and compare very favorably with those in **1**.[3]

The molecule exhibits dynamic behavior in solution that was revealed by its temperature-dependent ^1H NMR and ^{13}C NMR spectra. At −40 °C, resonances 2 and 3 (see above) are broadened. At −12 °C, they have coalesced, and at 23 °C they are observed as a slightly broadened singlet (3 H) at −18.76 ppm with weak coupling to platinum, $^2J_{Pt\text{-}H} \approx 25$ Hz. At the coalescence temperature, ΔG^*_{261} = 12.3 kcal/mol. The ^{13}C NMR spectrum of **2** at −49 °C shows eight resonances due to the carbonyl ligands.

(6) (a) Teller, R. G.; Bau, R. *Struct. Bonding* **1981**, *44*, 1. (b) Bau, R., Ed. *Transition Metal Hydrides*; Advances in Chemistry Series 167; American Chemical Society: Washington, DC, 1978.

Scheme I. Internal Rotation Mechanism[a]

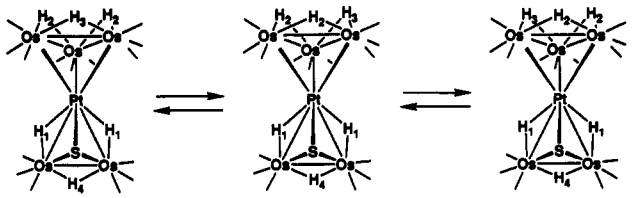

2

[a] Os_3 and Os_2S triangles rotate at Pt pivot.

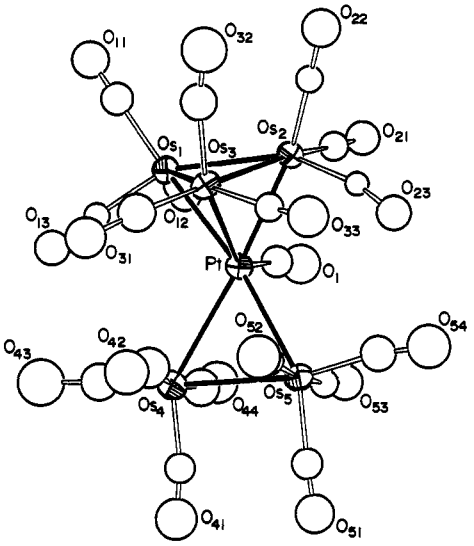

Figure 2. ORTEP diagram of $PtOs_5(CO)_{18}(\mu\text{-}H)_4$ (**3**) showing 50% probability thermal ellipsoids.

These lie at 174.69 (1 CO), 173.45 (2 CO), 168.6 (2 CO), 165.15 (2 CO), 164.36 (2 CO), 163.00 (2 CO), 162.79 (2 CO), and 157.47 (2 CO) ppm. This is consistent with the solid-state structure of the molecule. As the temperature is raised, the resonances at 174.69 and 173.45 ppm broaden and coalesce (≈−12 °C). At the same time, the three resonances at 165.15, 164.36, and 163.00 ppm also broaden and coalesce (≈−12 °C; resonances are in the baseline). The resonances at 168.60, 162.79, and 157.47 ppm exhibit no temperature-dependent changes. At 25 °C, the resonances from 174.69 and 173.45 ppm have re-formed as a slightly broadened singlet at 173.27 ppm (3 CO) which shows coupling to ^{195}Pt, $J_{Pt\text{-}C}$ = 36.4 Hz, and the resonances from 165.15, 164.36, and 163.00 ppm have re-formed as a broad singlet at 163.95 ppm (6 CO). ΔG^*_{261} equals 12.3 kcal/mol at the coalescence temperature, which indicates that the dynamic process observed in the ^1H NMR and ^{13}C NMR spectra is one and the same.

The proposed mechanism for this dynamic process consists of an intramolecular internal rotation of the Os_3 triangular grouping relative to the Os_2S triangle about the platinum atom; see Scheme I. In the course of this rearrangement, the hydride ligands H_2 and H_3 are averaged, while H_1 and H_4 are not. The CO ligands on the Os_3 triangle that are positioned trans to the platinum atom are averaged at the same rate. The averaging of the resonances at 174.69 and 173.45 ppm is attributed to the averaging of these ligands. Simultaneously, the six CO ligands on the Os_3 triangle that lie cis to the platinum atom are averaged. This is attributed to the averaging of the resonances at 165.15, 164.36, and 163.00 ppm.

Compound **1** was observed to react with $Os(CO)_5$ at 25 °C to yield two new compounds: $PtOs_5(CO)_{18}(\mu\text{-}H)_4$ (**3**), 38%, and $PtOs_4(CO)_{15}(\mu\text{-}H)_2$ (**4**), 25%. Both of these compounds were characterized by IR, ^1H NMR, and single-crystal X-ray diffraction analyses. An ORTEP diagram of the molecular structure of **3** is shown in Figure 2. Final atomic positional parameters are listed in Table V. Selected interatomic distances and angles are listed

Table II. Positional Parameters and B(eq) for $PtOs_5(CO)_{15}(S)(H)_6$ (2)

atom	x	y	z	B(eq), Å^2	atom	x	y	z	B(eq), Å^2
Pt(A)	0.03149 (08)	0.32821 (05)	0.47955 (13)	3.46 (5)	O(43C)	0.6946 (13)	0.5785 (09)	0.798 (02)	6 (1)
Pt(B)	0.25039 (07)	0.01684 (05)	0.15901 (12)	3.17 (5)	O(51A)	−0.0185 (17)	0.4751 (11)	0.334 (03)	9 (1)
Pt(C)	0.56141 (07)	0.34010 (04)	0.79181 (12)	2.89 (5)	O(51B)	0.4047 (15)	0.1431 (09)	0.105 (02)	7 (1)
Os(1A)	0.17199 (08)	0.38218 (05)	0.45425 (13)	3.60 (6)	O(51C)	0.7262 (16)	0.3085 (10)	0.597 (03)	8 (1)
Os(1B)	0.16380 (08)	0.09228 (05)	0.01021 (13)	3.89 (6)	O(52A)	−0.0706 (16)	0.4169 (10)	0.731 (02)	7 (1)
Os(1C)	0.47078 (08)	0.27696 (05)	0.53714 (12)	3.39 (5)	O(52B)	0.3774 (16)	0.0951 (09)	0.517 (02)	7 (1)
Os(2A)	0.14355 (08)	0.35324 (05)	0.72910 (14)	4.24 (6)	O(52C)	0.6844 (14)	0.2440 (10)	0.997 (03)	8 (1)
Os(2B)	0.13786 (08)	0.05598 (05)	0.28092 (13)	3.60 (6)	O(53A)	−0.2432 (19)	0.3963 (14)	0.336 (03)	11 (2)
Os(2C)	0.45786 (07)	0.23847 (05)	0.81233 (12)	3.20 (5)	O(53B)	0.5509 (15)	0.0260 (12)	0.347 (03)	8 (2)
Os(3A)	−0.08138 (09)	0.24800 (05)	0.49456 (14)	4.36 (6)	O(53C)	0.8615 (15)	0.4013 (12)	1.005 (03)	9 (2)
Os(3B)	0.29421 (08)	−0.07656 (05)	0.26864 (13)	3.45 (5)	C(11A)	0.276 (02)	0.3840 (13)	0.492 (03)	4.2 (7)
Os(3C)	0.60644 (07)	0.41067 (05)	1.03374 (12)	3.12 (5)	C(11B)	0.071 (02)	0.1077 (14)	−0.066 (04)	5.1 (8)
Os(4A)	−0.04989 (08)	0.28387 (05)	0.23065 (13)	3.67 (6)	C(11C)	0.372 (02)	0.2426 (13)	0.439 (04)	4.5 (7)
Os(4B)	0.31486 (08)	−0.04511 (05)	−0.00686 (13)	3.78 (6)	C(12A)	0.1655 (20)	0.3522 (13)	0.269 (04)	4.8 (7)
Os(4C)	0.62129 (07)	0.44956 (05)	0.76285 (13)	3.19 (5)	C(12B)	0.175 (02)	0.0679 (13)	−0.170 (04)	5.2 (8)
Os(5A)	−0.09430 (08)	0.36572 (05)	0.42492 (13)	3.85 (6)	C(12C)	0.4748 (19)	0.3402 (13)	0.421 (04)	4.6 (7)
Os(5B)	0.39258 (08)	0.02912 (05)	0.24802 (13)	3.67 (6)	C(13A)	0.186 (02)	0.4640 (16)	0.421 (04)	6.5 (9)
Os(5C)	0.70369 (08)	0.36311 (05)	0.87894 (14)	3.65 (6)	C(13B)	0.208 (02)	0.1712 (15)	0.017 (04)	5.2 (8)
S(1A)	0.1362 (05)	0.2847 (03)	0.5229 (08)	3.8 (3)	C(13C)	0.5150 (19)	0.2287 (12)	0.422 (03)	4.0 (7)
S(1B)	0.1268 (05)	−0.0059 (03)	0.0652 (08)	4.2 (4)	C(21A)	0.240 (03)	0.3477 (18)	0.820 (05)	8 (1)
S(1C)	0.4362 (05)	0.3303 (03)	0.7287 (08)	3.4 (3)	C(21B)	0.045 (02)	0.0613 (14)	0.257 (04)	5.2 (8)
O(11A)	0.3339 (15)	0.3848 (12)	0.509 (03)	8 (1)	C(21C)	0.357 (02)	0.1989 (12)	0.764 (03)	4.0 (7)
O(11B)	0.0145 (18)	0.1171 (12)	−0.106 (03)	9 (2)	C(22A)	0.1044 (19)	0.2913 (14)	0.834 (04)	4.6 (7)
O(11C)	0.3180 (14)	0.2229 (11)	0.377 (03)	8 (1)	C(22B)	0.1241 (19)	−0.0071 (14)	0.393 (04)	4.7 (7)
O(12A)	0.1645 (13)	0.3331 (10)	0.152 (02)	6 (1)	C(22C)	0.4464 (19)	0.2583 (12)	0.991 (04)	4.2 (7)
O(12B)	0.1777 (15)	0.0497 (10)	−0.287 (02)	7 (1)	C(23A)	0.137 (02)	0.4179 (15)	0.866 (04)	5.5 (8)
O(12C)	0.4737 (15)	0.3788 (08)	0.356 (02)	6 (1)	C(23B)	0.1671 (19)	0.1172 (13)	0.441 (04)	4.4 (7)
O(13A)	0.1886 (14)	0.5110 (09)	0.393 (03)	7 (1)	C(23C)	0.4945 (19)	0.1666 (13)	0.857 (03)	4.0 (7)
O(13B)	0.2396 (15)	0.2183 (10)	0.017 (03)	8 (1)	C(31A)	−0.020 (02)	0.1883 (14)	0.519 (03)	4.2 (7)
O(13C)	0.5454 (16)	0.2011 (09)	0.360 (02)	7 (1)	C(31B)	0.191 (02)	−0.1161 (13)	0.220 (03)	4.2 (7)
O(21A)	0.2949 (17)	0.3446 (14)	0.874 (03)	10 (2)	C(31C)	0.511 (02)	0.4218 (12)	1.029 (03)	3.6 (7)
O(21B)	−0.0200 (18)	0.0682 (12)	0.248 (03)	9 (2)	C(32A)	−0.0722 (19)	0.2694 (12)	0.691 (04)	4.3 (7)
O(21C)	0.3006 (14)	0.1768 (12)	0.743 (03)	8 (1)	C(32B)	0.2851 (17)	−0.0509 (11)	0.454 (03)	3.4 (6)
O(22A)	0.0814 (17)	0.2552 (10)	0.885 (03)	8 (1)	C(32C)	0.5999 (18)	0.3478 (12)	1.147 (03)	3.8 (7)
O(22B)	0.1122 (16)	−0.0451 (10)	0.461 (03)	7 (1)	C(33A)	−0.174 (03)	0.1955 (17)	0.471 (04)	7 (1)
O(22C)	0.4370 (14)	0.2742 (08)	1.104 (03)	7 (1)	C(33B)	0.3353 (19)	−0.1447 (14)	0.326 (03)	4.2 (7)
O(23A)	0.1334 (19)	0.4572 (11)	0.940 (03)	10 (2)	C(33C)	0.6497 (17)	0.4731 (12)	1.191 (03)	3.1 (6)
O(23B)	0.1832 (15)	0.1530 (09)	0.527 (02)	7 (1)	C(41A)	0.0155 (19)	0.2322 (12)	0.204 (03)	3.5 (6)
O(23C)	0.5155 (16)	0.1247 (10)	0.871 (03)	8 (1)	C(41B)	0.2226 (19)	−0.0808 (12)	−0.122 (03)	3.6 (7)
O(31A)	0.0147 (17)	0.1530 (10)	0.541 (03)	8 (2)	C(41C)	0.526 (02)	0.4679 (14)	0.700 (04)	4.7 (8)
O(31B)	0.1383 (14)	−0.1387 (09)	0.205 (03)	7 (1)	C(42A)	−0.0043 (17)	0.3439 (12)	0.136 (03)	3.4 (6)
O(31C)	0.4549 (14)	0.4266 (09)	1.032 (03)	6 (1)	C(42B)	0.331 (02)	0.0174 (15)	−0.122 (04)	5.7 (8)
O(32A)	−0.0661 (18)	0.2831 (11)	0.809 (02)	9 (2)	C(42C)	0.630 (02)	0.4303 (14)	0.565 (04)	5.2 (8)
O(32B)	0.2801 (14)	−0.0322 (09)	0.565 (02)	6 (1)	C(43A)	−0.124 (02)	0.2509 (15)	0.068 (04)	5.6 (8)
O(32C)	0.5985 (14)	0.3111 (08)	1.218 (02)	6 (1)	C(43B)	0.3622 (20)	−0.0966 (13)	−0.107 (03)	4.4 (7)
O(33A)	−0.2256 (18)	0.1668 (12)	0.460 (03)	11 (2)	C(43C)	0.6662 (16)	0.5283 (12)	0.780 (03)	2.9 (6)
O(33B)	0.3590 (18)	−0.1855 (09)	0.355 (03)	9 (2)	C(51A)	−0.051 (02)	0.4322 (16)	0.375 (04)	7 (1)
O(33C)	0.6769 (13)	0.5087 (09)	1.276 (02)	7 (1)	C(51B)	0.402 (02)	0.1009 (14)	0.160 (04)	5.3 (8)
O(41A)	0.0553 (16)	0.2033 (10)	0.189 (03)	7 (1)	C(51C)	0.716 (02)	0.3284 (15)	0.703 (04)	6.2 (9)
O(41B)	0.1686 (15)	−0.1039 (11)	−0.183 (03)	8 (1)	C(52A)	−0.0804 (20)	0.4000 (13)	0.616 (04)	4.8 (7)
O(41C)	0.4741 (16)	0.4801 (09)	0.667 (03)	7 (1)	C(52B)	0.3829 (19)	0.0702 (13)	0.242 (04)	4.1 (7)
O(42A)	0.0224 (13)	0.3779 (09)	0.077 (02)	6 (1)	C(52C)	0.695 (02)	0.2866 (17)	0.959 (04)	7 (1)
O(42B)	0.3405 (15)	0.0559 (09)	−0.186 (02)	7 (1)	C(53A)	−0.187 (02)	0.3812 (15)	0.373 (04)	6.2 (9)
O(42C)	0.6350 (14)	0.4130 (10)	0.459 (02)	7 (1)	C(53B)	0.492 (02)	0.0267 (14)	0.305 (04)	5.0 (8)
O(43A)	−0.1687 (15)	0.2312 (11)	−0.026 (03)	8 (1)	C(53C)	0.805 (02)	0.3893 (14)	0.954 (04)	4.9 (8)
O(43B)	0.3931 (17)	−0.1248 (11)	−0.167 (03)	9 (2)					

in Tables VI and VII. The cluster of this molecule is similar to that of **2**, a $PtOs_3$ tetrahedron fused to a $PtOs_2$ triangle via the platinum atom. The metal atoms of the Os_3 triangle each contain three linear terminal carbonyl ligands. Os(4) and Os(5) have four and the platinum atom has one. The molecule contains four bridging hydride ligands, as indicated by its ^{1}H NMR spectrum. These ligands were not observed directly in the structural analysis, but at −65 °C, the ^{1}H NMR spectrum of **3** exhibits four hydride resonances: (1) −17.41 ppm (s, 1 H) with strong coupling to ^{195}Pt, $^1J_{Pt-H}$ = 436.0 Hz; (2) −18.09 ppm (s, 1 H) with strong coupling to platinum, $^1J_{Pt-H}$ = 438.6 Hz; (3) −18.14 ppm (s, 1 H) with no coupling to platinum; and (4) −18.53 ppm (s, 1 H) with no coupling to platinum. On the basis of the strong coupling to platinum, it is concluded that resonances 1 and 2 are due to hydride ligands bonded directly to Pt. In support of this, the structural analysis shows that two of the Pt–Os bonds are unusually long, Pt–Os(4) = 3.052 (3) Å vs Pt–Os(5) = 2.859 (3) Å and Pt–Os(3) = 2.912 (3) Å vs Pt–Os(1) = 2.762 (3) Å and Pt–Os(2) = 2.729 (3) Å. Thus, we believe hydride ligands bridge the Pt–Os(4) and Pt–Os(3) bonds. In addition, two of the Os–Os distances in the Os_3 triangle are significantly longer than the third, Os(1)–Os(2) = 2.906 (3) Å and Os(1)–Os(3) = 2.925 (3) Å vs Os(2)–Os(3) = 2.769 (3) Å. Accordingly, we believe that hydride ligands bridge the Os(1)–Os(2) and Os(1)–Os(3) bonds and are attributed to resonances 3 and 4. At temperatures above −65 °C, all of the resonances broaden, and at 25 °C, they collapse into the baseline. Clearly, there is a dynamic process that is averaging the environments of all of the hydride ligands. We believe that this is simply a form of migratory hydride scrambling that is well-known to occur in hydride-containing metal carbonyl cluster complexes.[7]

An ORTEP drawing of the molecular structure of **4** is shown in Figure 3. Final atomic positional parameters are listed in Table VIII. Selected interatomic distances and angles are listed in Table

(7) Band, E.; Muetterties, E. L. *Chem. Rev.* **1978**, *78*, 639.

Table III. Intramolecular Distances for **2**[a]

Pt(A)–Os(1A)	2.886 (2)	Os(2C)–S(1C)	2.400 (7)
Pt(A)–Os(2A)	2.901 (2)	Os(2C)–C(21C)	1.98 (4)
Pt(A)–Os(3A)	2.679 (2)	Os(2C)–C(22C)	1.84 (3)
Pt(A)–Os(4A)	2.667 (2)	Os(2C)–C(23C)	1.95 (3)
Pt(A)–Os(5A)	2.695 (2)	Os(3A)–Os(4A)	2.915 (2)
Pt(A)–S(1A)	2.39 (1)	Os(3A)–Os(5A)	2.890 (2)
Pt(B)–Os(1B)	2.895 (2)	Os(3A)–C(31A)	1.96 (4)
Pt(B)–Os(2B)	2.905 (2)	Os(3A)–C(32A)	1.91 (3)
Pt(B)–Os(3B)	2.669 (2)	Os(3A)–C(33A)	1.97 (4)
Pt(B)–Os(4B)	2.680 (2)	Os(3B)–Os(4B)	2.928 (2)
Pt(B)–Os(5B)	2.702 (2)	Os(3B)–Os(5B)	2.903 (2)
Pt(B)–S(1B)	2.37 (1)	Os(3B)–C(31B)	2.02 (4)
Pt(C)–Os(1C)	2.897 (2)	Os(3B)–C(32B)	1.90 (3)
Pt(C)–Os(2C)	2.892 (2)	Os(3B)–C(33B)	1.95 (4)
Pt(C)–Os(3C)	2.676 (2)	Os(3C)–Os(4C)	2.914 (2)
Pt(C)–Os(4C)	2.673 (2)	Os(3C)–Os(5C)	2.918 (2)
Pt(C)–Os(5C)	2.693 (2)	Os(3C)–C(31C)	1.91 (4)
Pt(C)–S(1C)	2.367 (9)	Os(3C)–C(32C)	1.90 (3)
Os(1A)–Os(2A)	2.950 (2)	Os(3C)–C(33C)	1.98 (3)
Os(1A)–S(1A)	2.435 (7)	Os(4A)–Os(5A)	2.907 (2)
Os(1A)–C(11A)	1.98 (4)	Os(4A)–C(41A)	1.91 (4)
Os(1A)–C(12A)	1.86 (4)	Os(4A)–C(42A)	1.92 (3)
Os(1A)–C(13A)	1.93 (4)	Os(4A)–C(43A)	1.95 (4)
Os(1B)–Os(2B)	2.947 (2)	Os(4B)–Os(5B)	2.917 (2)
Os(1B)–S(1B)	2.403 (7)	Os(4B)–C(41B)	1.95 (4)
Os(1B)–C(11B)	1.92 (5)	Os(4B)–C(42B)	1.93 (4)
Os(1B)–C(12B)	1.87 (4)	Os(4B)–C(43B)	1.92 (4)
Os(1B)–C(13B)	1.88 (3)	Os(4C)–Os(5C)	2.918 (2)
Os(1C)–Os(2C)	2.942 (2)	Os(4C)–C(41C)	1.96 (4)
Os(1C)–S(1C)	2.412 (7)	Os(4C)–C(42C)	2.00 (4)
Os(1C)–C(11C)	1.99 (4)	Os(4C)–C(43C)	1.87 (3)
Os(1C)–C(12C)	1.92 (3)	Os(5A)–C(51A)	1.78 (4)
Os(1C)–C(13C)	1.92 (4)	Os(5A)–C(52A)	1.92 (4)
Os(2A)–S(1A)	2.425 (8)	Os(5A)–C(53A)	1.87 (5)
Os(2A)–C(21A)	1.95 (6)	Os(5B)–C(51B)	1.93 (3)
Os(2A)–C(22A)	1.97 (3)	Os(5B)–C(52B)	1.95 (3)
Os(2A)–C(23A)	1.95 (4)	Os(5B)–C(53B)	1.92 (4)
Os(2B)–S(1B)	2.402 (8)	Os(5C)–C(51C)	1.91 (4)
Os(2B)–C(21B)	1.81 (4)	Os(5C)–C(52C)	1.98 (4)
Os(2B)–C(22B)	1.91 (3)	Os(5C)–C(53C)	1.96 (4)
Os(2B)–C(23B)	1.95 (3)	O–C(av)	1.14 (5)

[a] Distances are in angstroms. Estimated standard deviations in the least significant figure are given in parentheses.

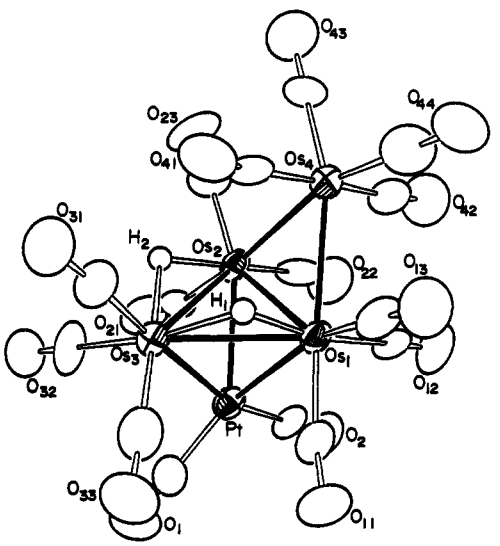

Figure 3. ORTEP diagram of $PtOs_4(CO)_{15}(\mu\text{-}H)_2$ (**4**) showing 50% probability thermal ellipsoids.

IX and X. The cluster consists of a $PtOs_3$ tetrahedral group with an $Os(CO)_4$ grouping bridging the Os(1)–Os(2) bond. The molecule has an approximate reflection symmetry (not crystallographically imposed) with the metal atoms Pt, Os(3) and Os(4) lying on the reflection plane. The molecule contains two symmetry-equivalent hydride ligands (located crystallographically, but not refined) that bridge the elongated Os(1)–Os(3) and

Table IV. Intramolecular Bond Angles for **2**[a]

Os(1A)–Pt(A)–Os(2A)	61.28 (5)	Os(2B)–Os(1B)–S(1B)	52.1 (2)
Os(1A)–Pt(A)–Os(3A)	162.28 (7)	Pt(C)–Os(1C)–Os(2C)	59.37 (4)
Os(1A)–Pt(A)–Os(4A)	111.81 (6)	Pt(C)–Os(1C)–S(1C)	52.0 (2)
Os(1A)–Pt(A)–Os(5A)	131.36 (6)	Os(2C)–Os(1C)–S(1C)	52.1 (2)
Os(1A)–Pt(A)–S(1A)	54.0 (2)	Pt(A)–Os(2A)–Os(1A)	59.11 (5)
Os(2A)–Pt(A)–Os(3A)	115.70 (6)	Pt(A)–Os(2A)–S(1A)	52.4 (2)
Os(2A)–Pt(A)–Os(4A)	164.24 (7)	Os(1A)–Os(2A)–S(1A)	52.8 (2)
Os(2A)–Pt(A)–Os(5A)	129.93 (6)	Pt(B)–Os(2B)–Os(1B)	59.30 (5)
Os(2A)–Pt(A)–S(1A)	53.5 (2)	Pt(B)–Os(2B)–S(1B)	51.9 (2)
Os(3A)–Pt(A)–Os(4A)	66.08 (5)	Os(1B)–Os(2B)–S(1B)	52.2 (2)
Os(3A)–Pt(A)–Os(5A)	65.08 (6)	Pt(C)–Os(2C)–Os(1C)	59.53 (4)
Os(3A)–Pt(A)–S(1A)	109.3 (2)	Pt(C)–Os(2C)–S(1C)	52.1 (2)
Os(4A)–Pt(A)–Os(5A)	65.66 (6)	Os(1C)–Os(2C)–S(1C)	52.5 (2)
Os(4A)–Pt(A)–S(1A)	110.8 (2)	Pt(A)–Os(3A)–Os(4A)	56.78 (5)
Os(5A)–Pt(A)–S(1A)	174.0 (2)	Pt(A)–Os(3A)–Os(5A)	57.73 (5)
Os(1B)–Pt(B)–Os(2B)	61.07 (5)	Os(4A)–Os(3A)–Os(5A)	60.10 (4)
Os(1B)–Pt(B)–Os(3B)	162.61 (6)	Pt(B)–Os(3B)–Os(4B)	56.99 (5)
Os(1B)–Pt(B)–Os(4B)	113.25 (6)	Pt(B)–Os(3B)–Os(5B)	57.83 (5)
Os(1B)–Pt(B)–Os(5B)	131.28 (6)	Os(4B)–Os(3B)–Os(5B)	60.04 (5)
Os(1B)–Pt(B)–S(1B)	53.2 (2)	Pt(C)–Os(3C)–Os(4C)	56.95 (4)
Os(2B)–Pt(B)–Os(3B)	112.81 (6)	Pt(C)–Os(3C)–Os(5C)	57.36 (5)
Os(2B)–Pt(B)–Os(4B)	159.94 (6)	Os(4C)–Os(3C)–Os(5C)	60.04 (5)
Os(2B)–Pt(B)–Os(5B)	133.52 (6)	Pt(A)–Os(4A)–Os(3A)	57.15 (5)
Os(2B)–Pt(B)–S(1B)	53.0 (2)	Pt(A)–Os(4A)–Os(5A)	57.62 (5)
Os(3B)–Pt(B)–Os(4B)	66.37 (5)	Os(3A)–Os(4A)–Os(5A)	59.54 (5)
Os(3B)–Pt(B)–Os(5B)	65.44 (5)	Pt(B)–Os(4B)–Os(3B)	56.64 (5)
Os(3B)–Pt(B)–S(1B)	109.6 (2)	Pt(B)–Os(4B)–Os(5B)	57.54 (5)
Os(4B)–Pt(B)–Os(5B)	65.65 (6)	Os(3B)–Os(4B)–Os(5B)	59.57 (4)
Os(4B)–Pt(B)–S(1B)	107.5 (2)	Pt(C)–Os(4C)–Os(3C)	57.03 (4)
Os(5B)–Pt(B)–S(1B)	172.5 (2)	Pt(C)–Os(4C)–Os(5C)	57.39 (5)
Os(1C)–Pt(C)–Os(2C)	61.10 (4)	Os(3C)–Os(4C)–Os(5C)	60.05 (5)
Os(1C)–Pt(C)–Os(3C)	161.60 (7)	Pt(A)–Os(5A)–Os(3A)	57.19 (5)
Os(1C)–Pt(C)–Os(4C)	113.98 (6)	Pt(A)–Os(5A)–Os(4A)	56.72 (5)
Os(1C)–Pt(C)–Os(5C)	132.00 (6)	Os(3A)–Os(5A)–Os(4A)	60.37 (4)
Os(1C)–Pt(C)–S(1C)	53.4 (2)	Pt(B)–Os(5B)–Os(3B)	56.73 (5)
Os(2C)–Pt(C)–Os(3C)	112.78 (5)	Pt(B)–Os(5B)–Os(4B)	56.81 (5)
Os(2C)–Pt(C)–Os(4C)	162.24 (7)	Os(3B)–Os(5B)–Os(4B)	60.39 (4)
Os(2C)–Pt(C)–Os(5C)	130.97 (6)	Pt(C)–Os(5C)–Os(3C)	56.79 (5)
Os(2C)–Pt(C)–S(1C)	53.2 (2)	Pt(C)–Os(5C)–Os(4C)	56.74 (5)
Os(3C)–Pt(C)–Os(4C)	66.01 (4)	Os(3C)–Os(5C)–Os(4C)	59.91 (5)
Os(3C)–Pt(C)–Os(5C)	65.85 (5)	Pt(A)–S(1A)–Os(1A)	73.5 (2)
Os(3C)–Pt(C)–S(1C)	108.5 (2)	Pt(A)–S(1A)–Os(2A)	74.1 (2)
Os(4C)–Pt(C)–Os(5C)	65.87 (5)	Os(1A)–S(1A)–Os(2A)	74.7 (2)
Os(4C)–Pt(C)–S(1C)	109.5 (2)	Pt(B)–S(1B)–Os(1B)	74.8 (2)
Os(5C)–Pt(C)–S(1C)	173.6 (2)	Pt(B)–S(1B)–Os(2B)	75.1 (2)
Pt(A)–Os(1A)–Os(2A)	59.61 (5)	Os(1B)–S(1B)–Os(2B)	75.7 (2)
Pt(A)–Os(1A)–S(1A)	52.5 (2)	Pt(C)–S(1C)–Os(1C)	74.6 (2)
Os(2A)–Os(1A)–S(1A)	52.5 (2)	Pt(C)–S(1C)–Os(2C)	74.7 (3)
Pt(B)–Os(1B)–Os(2B)	59.63 (5)	Os(1C)–S(1C)–Os(2C)	75.4 (2)
Pt(B)–Os(1B)–S(1B)	52.0 (2)	Os–C(av)–O	176 (4)

[a] Angles are in degrees. Estimated standard deviations in the least significant figure are given in parentheses.

Scheme II

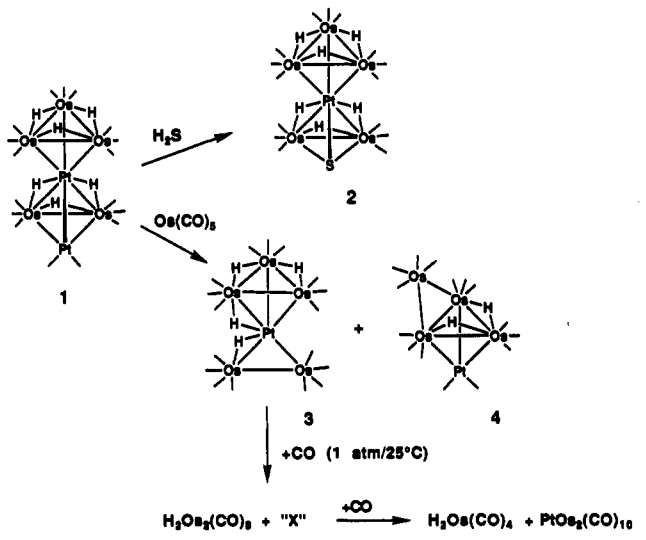

Os(2)–Os(3) metal–metal bonds, $\delta = -20.67$ ppm (s, 2 H). The platinum atom has two carbonyl ligands that appear to influence the Pt–Os bonding. In particular, the Pt–Os(3) bond that lies approximately opposite to the carbonyl ligand C(2)–O(2) is significantly shorter, 2.703 (1) Å, than the other Pt–Os bonds,

Table V. Positional Parameters and B(eq) for $PtOs_5(CO)_{18}(H)_4$ (3)

atom	x	y	z	B(eq), Å^2
Pt	0.3883 (02)	−0.0100	0.79571 (19)	2.18 (7)
Os(1)	0.3423 (02)	−0.10643 (16)	0.98909 (18)	2.31 (7)
Os(2)	0.4505 (03)	−0.14327 (15)	0.74851 (19)	2.38 (8)
Os(3)	0.1159 (02)	−0.10879 (15)	0.64757 (19)	2.38 (7)
Os(4)	0.2917 (03)	0.13407 (16)	0.8536 (02)	2.99 (9)
Os(5)	0.3909 (03)	0.10194 (15)	0.5995 (02)	2.79 (8)
O(1)	0.768 (06)	−0.003 (02)	0.986 (04)	6 (1)
O(11)	0.275 (05)	−0.221 (02)	1.172 (04)	5.3 (9)
O(12)	0.676 (05)	−0.0636 (19)	1.256 (04)	4.1 (8)
O(13)	0.143 (05)	−0.005 (02)	1.088 (04)	4.5 (8)
O(21)	0.838 (05)	−0.1594 (20)	0.918 (04)	4.5 (8)
O(22)	0.386 (05)	−0.293 (02)	0.642 (04)	5 (1)
O(23)	0.427 (04)	−0.100 (02)	0.428 (04)	4.3 (7)
O(31)	−0.216 (06)	−0.047 (02)	0.628 (04)	6 (1)
O(32)	0.029 (07)	−0.260 (03)	0.608 (05)	7 (1)
O(33)	0.056 (05)	−0.099 (02)	0.306 (04)	6 (1)
O(41)	0.247 (06)	0.281 (03)	0.757 (05)	6 (1)
O(42)	−0.073 (06)	0.102 (03)	0.621 (05)	7 (1)
O(43)	0.179 (07)	0.155 (03)	1.117 (05)	8 (1)
O(44)	0.663 (07)	0.149 (03)	1.089 (05)	7 (1)
O(51)	0.352 (05)	0.248 (02)	0.477 (04)	6 (1)
O(52)	0.028 (06)	0.062 (02)	0.368 (05)	6 (1)
O(53)	0.769 (05)	0.125 (02)	0.824 (04)	4.9 (9)
O(54)	0.506 (06)	0.046 (02)	0.366 (05)	7 (1)
C(1)	0.622 (07)	−0.009 (03)	0.917 (05)	4 (1)
C(11)	0.287 (07)	−0.180 (03)	1.094 (06)	4 (1)
C(12)	0.554 (07)	−0.080 (03)	1.160 (05)	3 (1)
C(13)	0.224 (06)	−0.046 (02)	1.053 (05)	2 (1)
C(21)	0.685 (07)	−0.151 (03)	0.852 (05)	3 (1)
C(22)	0.411 (06)	−0.233 (03)	0.682 (05)	3 (1)
C(23)	0.446 (05)	−0.124 (02)	0.553 (05)	1.9 (8)
C(31)	−0.081 (08)	−0.076 (03)	0.633 (06)	5 (1)
C(32)	0.060 (08)	−0.201 (03)	0.637 (06)	5 (1)
C(33)	0.081 (06)	−0.099 (03)	0.435 (05)	2.8 (9)
C(41)	0.271 (07)	0.225 (03)	0.785 (05)	3 (1)
C(42)	0.060 (09)	0.102 (04)	0.694 (07)	6 (1)
C(43)	0.234 (08)	0.144 (03)	1.004 (06)	5 (1)
C(44)	0.531 (09)	0.149 (04)	1.006 (08)	5 (1)
C(51)	0.365 (07)	0.195 (03)	0.525 (06)	3 (1)
C(52)	0.153 (06)	0.073 (03)	0.456 (05)	3 (1)
C(53)	0.623 (06)	0.120 (03)	0.746 (05)	3 (1)
C(54)	0.459 (08)	0.062 (03)	0.456 (06)	5 (1)

Table VI. Intramolecular Distances for 3[a]

Pt–Os(1)	2.762 (3)	Os(2)–C(23)	1.85 (4)
Pt–Os(2)	2.729 (3)	Os(3)–C(31)	1.81 (7)
Pt–Os(3)	2.912 (3)	Os(3)–C(32)	1.86 (7)
Pt–Os(4)	3.052 (3)	Os(3)–C(33)	1.88 (4)
Pt–Os(5)	2.859 (3)	Os(4)–Os(5)	2.950 (3)
Pt–C(1)	1.87 (5)	Os(4)–C(41)	1.86 (6)
Os(1)–Os(2)	2.906 (3)	Os(4)–C(42)	2.03 (7)
Os(1)–Os(3)	2.925 (3)	Os(4)–C(43)	1.71 (6)
Os(1)–C(11)	1.93 (6)	Os(4)–C(44)	1.98 (7)
Os(1)–C(12)	1.92 (5)	Os(5)–C(51)	1.92 (6)
Os(1)–C(13)	1.84 (5)	Os(5)–C(52)	2.01 (5)
Os(2)–Os(3)	2.769 (3)	Os(5)–C(53)	1.94 (5)
Os(2)–C(21)	1.87 (5)	Os(5)–C(54)	1.88 (6)
Os(2)–C(22)	1.84 (5)	O–C(av)	1.17 (7)

[a] Distances are in angstroms. Estimated standard deviations in the least significant figure are given in parentheses.

Table VII. Intramolecular Bond Angles for 3[a]

Os(1)–Pt–Os(2)	63.90 (8)	Pt–Os(1)–Os(3)	61.52 (7)
Os(1)–Pt–Os(3)	62.00 (7)	Os(2)–Os(1)–Os(3)	56.69 (7)
Os(1)–Pt–Os(4)	111.9 (1)	Pt–Os(2)–Os(1)	58.61 (7)
Os(1)–Pt–Os(5)	170.4 (1)	Pt–Os(2)–Os(3)	63.97 (7)
Os(2)–Pt–Os(3)	58.68 (8)	Os(1)–Os(2)–Os(3)	62.01 (7)
Os(2)–Pt–Os(4)	174.7 (1)	Pt–Os(3)–Os(1)	56.48 (7)
Os(2)–Pt–Os(5)	124.1 (1)	Pt–Os(3)–Os(2)	57.36 (7)
Os(3)–Pt–Os(4)	116.9 (1)	Os(1)–Os(3)–Os(2)	61.30 (7)
Os(3)–Pt–Os(5)	116.07 (8)	Pt–Os(4)–Os(5)	56.86 (7)
Os(4)–Pt–Os(5)	59.77 (8)	Pt–Os(5)–Os(4)	63.37 (8)
Pt–Os(1)–Os(2)	57.50 (7)	M–C(av)–O	173 (7)

[a] Angles are in degrees. Estimated standard deviations in the least significant figure are given in parentheses.

Table VIII. Positional Parameters and B(eq) for $PtOs_4(CO)_{15}(H)_2$ (4)

atom	x	y	z	B(eq), Å^2
Pt	0.70210 (05)	−0.12644 (09)	0.71875 (04)	3.00 (4)
Os(1)	0.84425 (05)	0.00147 (09)	0.63409 (04)	2.84 (4)
Os(2)	0.63802 (05)	0.10366 (09)	0.63456 (04)	2.83 (4)
Os(3)	0.76392 (05)	0.15506 (09)	0.75340 (04)	2.80 (4)
Os(4)	0.78015 (06)	0.23538 (10)	0.54281 (05)	3.56 (4)
O(1)	0.6986 (15)	−0.238 (02)	0.8598 (12)	8 (1)
O(2)	0.6412 (12)	−0.4084 (19)	0.6426 (10)	6 (1)
O(11)	0.9556 (10)	−0.2280 (19)	0.7209 (10)	6 (1)
O(12)	0.8081 (11)	−0.234 (02)	0.5265 (10)	7 (1)
O(13)	1.0482 (09)	0.091 (02)	0.5804 (10)	7 (1)
O(21)	0.4643 (10)	0.0171 (18)	0.7229 (11)	6 (1)
O(22)	0.5569 (12)	−0.132 (02)	0.5369 (10)	7 (1)
O(23)	0.5085 (10)	0.3648 (18)	0.5813 (11)	6 (1)
O(31)	0.8349 (12)	0.476 (02)	0.7892 (10)	7 (1)
O(32)	0.5927 (11)	0.1865 (20)	0.8516 (09)	6 (1)
O(33)	0.9026 (12)	0.002 (02)	0.8530 (10)	7 (1)
O(41)	0.8622 (12)	0.464 (02)	0.6442 (10)	6 (1)
O(42)	0.6998 (18)	0.008 (02)	0.4373 (11)	9 (1)
O(43)	0.6631 (13)	0.493 (02)	0.4788 (11)	7 (1)
O(44)	0.9646 (13)	0.288 (03)	0.4611 (12)	9 (1)
C(1)	0.6987 (15)	−0.193 (03)	0.8071 (14)	4 (1)
C(2)	0.6627 (12)	−0.301 (02)	0.6711 (12)	3 (1)
C(11)	0.9048 (11)	−0.145 (02)	0.6923 (12)	4 (1)
C(12)	0.8216 (14)	−0.143 (02)	0.5676 (14)	4 (1)
C(13)	0.9712 (14)	0.062 (02)	0.6012 (13)	4 (1)
C(21)	0.5338 (14)	0.037 (02)	0.6931 (12)	4 (1)
C(22)	0.5894 (15)	−0.040 (03)	0.5696 (14)	5 (1)
C(23)	0.5574 (13)	0.270 (03)	0.6003 (13)	4 (1)
C(31)	0.8102 (13)	0.351 (03)	0.7725 (13)	4 (1)
C(32)	0.6575 (15)	0.176 (03)	0.8156 (14)	5 (1)
C(33)	0.8522 (13)	0.062 (03)	0.8133 (14)	5 (1)
C(41)	0.8264 (15)	0.377 (02)	0.6100 (13)	4 (1)
C(42)	0.7274 (19)	0.087 (03)	0.4783 (16)	6 (2)
C(43)	0.7043 (15)	0.390 (03)	0.5026 (13)	5 (1)
C(44)	0.8970 (17)	0.267 (04)	0.4912 (19)	8 (2)
H(1)	0.8447	0.1472	0.6805	4.0
H(2)	0.6581	0.2323	0.6975	4.0

Table IX. Intramolecular Distances for 4[a]

Pt–C(1)	1.87 (3)	Os(2)–C(22)	1.93 (3)
Pt–C(2)	1.88 (2)	Os(2)–C(23)	1.94 (2)
Pt–Os(3)	2.703 (1)	Os(2)–Os(4)	2.903 (1)
Pt–Os(2)	2.772 (1)	Os(2)–Os(3)	2.945 (1)
Pt–Os(1)	2.800 (1)	Os(3)–H(1)	1.80
Os(1)–H(1)	1.60	Os(3)–H(2)	1.90
Os(1)–C(12)	1.87 (2)	Os(3)–C(33)	1.87 (3)
Os(1)–C(13)	1.90 (2)	Os(3)–C(31)	1.87 (2)
Os(1)–C(11)	1.92 (2)	Os(3)–C(32)	1.91 (2)
Os(1)–Os(4)	2.885 (1)	Os(4)–C(43)	1.88 (2)
Os(1)–Os(2)	2.894 (1)	Os(4)–C(44)	1.90 (2)
Os(1)–Os(3)	2.967 (1)	Os(4)–C(41)	1.94 (3)
Os(2)–H(2)	1.70	Os(4)–C(42)	1.97 (3)
Os(2)–C(21)	1.92 (2)	O–C(av)	1.15 (3)

[a] Distances are in angstroms. Estimated standard deviations in the least significant figure are given in parentheses.

Pt–Os(1) = 2.800 (1) Å and Pt–Os(2) = 2.772 (1) Å. Compound 4 is structurally similar to the compounds $Os_5(CO)_{15}L(\mu\text{-}H)_2$ (L = CO, $P(OMe)_3$, I^-) (6) that were prepared by the addition of L to $Os_5(CO)_{15}(\mu\text{-}H)_2$.[8]

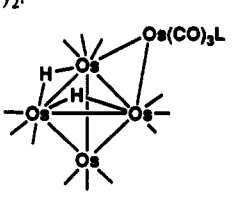

6

(8) (a) John, G. R.; Johnson, B. F. G.; Lewis, J.; Nelson, W. J.; McPartlin, M. *J. Organomet. Chem.* **1979**, *171*, C14. (b) Guy, J. J.; Sheldrick, G. M. *Acta Crystallogr.* **1978**, *B34*, 1725.

Table X. Intramolecular Bond Angles for 4[a]

C(1)–Pt–Os(2)	143.0 (7)	C(23)–Os(2)–Pt	159.4 (7)
C(1)–Pt–Os(1)	136.7 (6)	C(23)–Os(2)–Os(1)	139.2 (6)
C(2)–Pt–Os(3)	164.3 (7)	C(23)–Os(2)–Os(4)	80.5 (6)
C(2)–Pt–Os(2)	101.7 (7)	C(23)–Os(2)–Os(3)	118.8 (7)
C(2)–Pt–Os(1)	101.8 (7)	Pt–Os(2)–Os(1)	59.17 (3)
Os(3)–Pt–Os(2)	65.06 (3)	Pt–Os(2)–Os(4)	118.84 (3)
Os(3)–Pt–Os(1)	65.25 (3)	Pt–Os(2)–Os(3)	56.33 (3)
Os(2)–Pt–Os(1)	62.59 (3)	Os(1)–Os(2)–Os(4)	59.69 (3)
C(12)–Os(1)–Pt	93.2 (6)	Os(1)–Os(2)–Os(3)	61.08 (3)
C(12)–Os(1)–Os(4)	89.2 (6)	Os(4)–Os(2)–Os(3)	94.89 (3)
C(12)–Os(1)–Os(2)	93.9 (6)	C(33)–Os(3)–Pt	87.2 (7)
C(12)–Os(1)–Os(3)	146.4 (6)	C(33)–Os(3)–Os(2)	143.8 (8)
C(13)–Os(1)–Pt	159.4 (7)	C(33)–Os(3)–Os(1)	95.3 (7)
C(13)–Os(1)–Os(4)	80.6 (7)	C(31)–Os(3)–Pt	176.6 (8)
C(13)–Os(1)–Os(2)	139.8 (6)	C(31)–Os(3)–Os(2)	119.6 (7)
C(13)–Os(1)–Os(3)	119.0 (7)	C(31)–Os(3)–Os(1)	117.8 (7)
C(11)–Os(1)–Pt	68.9 (5)	C(32)–Os(3)–Pt	91.8 (7)
C(11)–Os(1)–Os(4)	172.3 (5)	C(32)–Os(3)–Os(2)	97.3 (8)
C(11)–Os(1)–Os(2)	127.0 (5)	C(32)–Os(3)–Os(1)	148.4 (7)
C(11)–Os(1)–Os(3)	88.0 (6)	Pt–Os(3)–Os(2)	58.61 (3)
Pt–Os(1)–Os(4)	118.52 (3)	Pt–Os(3)–Os(1)	58.96 (3)
Pt–Os(1)–Os(2)	58.24 (3)	Os(2)–Os(3)–Os(1)	58.62 (3)
Pt–Os(1)–Os(3)	55.80 (3)	C(43)–Os(4)–Os(1)	161.6 (7)
Os(4)–Os(1)–Os(2)	60.30 (3)	C(43)–Os(4)–Os(2)	102.3 (7)
Os(4)–Os(1)–Os(3)	94.78 (4)	C(44)–Os(4)–Os(1)	102.4 (9)
Os(2)–Os(1)–Os(3)	60.30 (3)	C(44)–Os(4)–Os(2)	162.0 (9)
C(21)–Os(2)–Pt	67.7 (6)	C(41)–Os(4)–Os(1)	85.7 (6)
C(21)–Os(2)–Os(1)	126.8 (6)	C(41)–Os(4)–Os(2)	91.0 (6)
C(21)–Os(2)–Os(4)	173.2 (6)	C(42)–Os(4)–Os(1)	92.7 (8)
C(21)–Os(2)–Os(3)	87.6 (7)	C(42)–Os(4)–Os(2)	85.6 (8)
C(22)–Os(2)–Pt	92.0 (6)	Os(1)–Os(4)–Os(2)	60.00 (3)
C(22)–Os(2)–Os(1)	96.1 (6)	O(11)–C(11)–Os(1)	168 (2)
C(22)–Os(2)–Os(4)	92.7 (7)	O(21)–C(21)–Os(2)	169 (2)
C(22)–Os(2)–Os(3)	146.9 (6)	O–C(av)–M	176 (2)

[a] Angles are in degrees. Estimated standard deviations in the least significant figure are given in parentheses.

The reaction of compound **3** with CO at 25 °C in $CDCl_3$ solvent was studied by performing the reaction in an NMR tube containing CO and by following the changes by ^1H NMR spectroscopy. Within 30 min, nearly all of compound **3** was gone. Substantial amounts of $H_2Os_2(CO)_8$[9] and $H_2Os(CO)_4$[10] in a 2/1 ratio were present together with an unidentified compound X that exhibits a resonance at −19.09 ppm with platinum satellites, J_{Pt-H} = 23 Hz. This compound was also observed as an intermediate in the CO-induced decomposition of **1**, but it could not be isolated.[3] It was suggested that X may be $PtOs_3(CO)_{12}(\mu\text{-}H)_2$,[11] which has been partially characterized previously. Phosphine derivatives of $PtOs_3(CO)_{12}(\mu\text{-}H)_2$ are known.[12] With longer exposure to CO, the intermediate was degraded and $H_2Os(CO)_4$ and $PtOs_2(CO)_{10}$ were formed.[4] Compounds **2** and **4** showed no significant decomposition in the presence of CO at 1 atm/25 °C over a 17-h period.

Discussion

A summary of the reactions performed in this study is shown in Scheme II. In the reactions of **1** both with H_2S and $Os(CO)_5$, the $Pt(CO)_2$ grouping was eliminated. Its fate has not been established in this study. In the reaction with $Os(CO)_5$, two hydride ligands were also eliminated and three CO ligands were added to form the product **3**. Product **4** was also formed in this reaction by the loss of four of the six hydride ligands, one mononuclear platinum grouping, and one mononuclear osmium grouping. Compound **3** was degraded by CO through cleavage of a molecule of $H_2Os_2(CO)_8$. The remaining platinum-containing grouping, which may be the compound $PtOs_3(CO)_{12}(\mu\text{-}H)_2$, was subsequently degraded by CO to $H_2Os(CO)_4$ and $PtOs_2(CO)_{10}$. Compound **1** is degraded by CO in a similar fashion.[3]

Compound **2** was found to exhibit a novel dynamic behavior in which the Os_3 and Os_2S triangular groupings rotate relative to one another on the platinum atom, which functions something like an atomic "ball bearing"; see Scheme I. The ^1H NMR spectrum of **1** indicated the existence of a similar dynamic process also, but we were unable to detect evidence for a slowing of the process by ^1H NMR spectroscopy even at −90 °C.[3]

Acknowledgment. These studies were supported by the National Science Foundation. The Bruker AM-500 NMR spectrometer was purchased with funds from the National Science Foundation under Grant No. CHE-8904942.

Supplementary Material Available: Tables of anisotropic thermal parameters (6 pages); listings of structure factor amplitudes (65 pages). Ordering information is given on any current masthead page.

(9) Moss, J. R.; Graham, W. A. G. *Inorg. Chem.* **1977**, *16*, 75.
(10) L'Eplattenier, F.; Calderazzo, F. *Inorg. Chem.* **1967**, *6*, 2092.
(11) Ewing, P.; Farrugia, L. J. *J. Organomet. Chem.* **1988**, *347*, C31.
(12) (a) Farrugia, L. J.; Howard, J. A. K.; Mitrprachachon, P.; Stone, F. G. A.; Woodward, P. *J. Chem. Soc., Dalton Trans.* **1981**, 162. (b) Farrugia, L. J. *Acta Crystallogr.* **1988**, *C44*, 1307. (c) Farrugia, L. J.; Green, M.; Hankey, D. R.; Murray, M.; Orpen, A. G.; Stone, F. G. A. *J. Chem. Soc., Dalton Trans.* **1985**, 177.